Preparation of Structurally Well-Defined Polymer−Nanoparticle Hybrids with Controlled/ Living Radical Polymerizations

Timothy von Werne and Timothy E. Patten*

Department of Chemistry
University of California at Davis
One Shields Avenue, Davis, California 95616-5295

The assembly of nanoparticles into organized structures yields materials with novel properties and also is an important step in exploiting the optical and magnetic properties of nanoparticles.[1−3] Spherical nanoparticles can be assembled into periodic, close-packed layers using sedimentation or slow crystallization procedures,[4,5] and these arrays act as Bragg gratings and diffract light of specific wavelengths.[6] Such materials could be developed into diffractive optics and photonic band gap materials. Other nanoparticle assembly methods have been investigated, including the use of DNA conjugates,[7−9] assembly onto monolayer surfaces,[10,11] electrostatic layer-by-layer formation,[12] templated crystallization,[13] and self-assembly of block copolymers[14] to define the spatial relationships of the nanoparticles. In only a few of these methods can the interparticle spacing be controlled.

We report the synthesis of structurally well-defined polymer−nanoparticle hybrids through integrating colloid and nanoparticle syntheses with recently reported controlled/living radical polymerizations.[15,16] In this method, atom transfer radical polymerization (ATRP)[17−19] is used to conduct a controlled/living polymerization from the surface of a silica nanoparticle macroinitiator, yielding a nanoparticle with an inorganic core and an outer layer of covalently attached, well-defined polymer chains (Scheme 1). Previous hybrid polymer/nanoparticle work also employed silica nanoparticles, but the methods involved grafting to[20−22] and through[23−27] the surfaces. By using a controlled/living polymerization to graft polymer chains from the nanoparticle surface, one can manipulate the structure of the resulting composite film through changes in the polymer's grafting density, composition,

Scheme 1. Synthetic Scheme for Structurally Well-Defined Polymer−Nanoparticle Hybrids
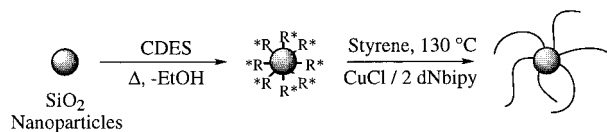
structure, and molar mass. For these reasons, grafting from flat and porous silica surfaces using controlled/living radical polymerizations is being investigated presently by several groups.[28−30]

Spherical silica particles, or Stöber silica,[31] with an average diameter of 70 nm, determined from TEM micrographs and dynamic light-scattering (DLS) measurements, were used for these experiments. The surface ATRP initiator, (2-(4-chloromethylphenyl)ethyl)dimethylethoxysilane (CDES), was deposited on the surface of the nanoparticles using a neat siloxane mixture in order to minimize the solvolysis of CDES by ethanol. After isolation and pentane washes, the resulting surface-modified particles could be redispersed in organic solvents. TEM micrographs and DLS measurements of the CDES-modified nanoparticles showed that the nanoparticles remained unagglomerated. Diffuse reflectance infrared Fourier transform (DRIFT) spectra of the CDES-modified nanoparticles showed sharp vibration bands at 3000−2870 and 1400−1500 cm^{-1} that were diagnostic for aromatic and alkyl groups and were not present in the DRIFT spectra of the starting nanoparticles. Elemental analyses indicated that the starting nanoparticles contained <0.05% chlorine and that the CDES-modified nanoparticles contained, on average, 0.51% chlorine. This difference translates into an average of 0.14 mmol initiator/g of silica particles and a grafting density of 2.6 CDES per nm^2. The latter number can be compared to the generally accepted silica surface hydroxyl group density, 5 hydroxyl groups per nm^2.[32] Such a grafting density would be expected, because the CDES group is much larger than a hydroxyl group and, consequently, would occupy more surface area per unit.

The surface-modified nanoparticles, thus prepared, were then used as macroinitiators for styrene ATRP (Table 1). Upon workup of a given sample, a white powder was obtained that dispersed easily in good solvents for polystyrene, and FTIR spectra of the product showed vibration bands corresponding to both polystyrene and silica. DLS measurements on these samples showed an increase in hydrodynamic diameter as a function of conversion (Table 1). It is known that when polymer chains are densely grafted to a surface, steric crowding will force the chains to stretch away from the surface. Therefore, the thickness of the polymer layer will be larger than twice the radius of gyration for the equivalent free polymer in solution.[33] Thus, the measured

(1) Alivisatos, A. P. *Science* **1996**, *271*, 933−937.
(2) Asher, S. A.; Holtz, J.; Weissman, J.; Pan, G. *Mater. Res. Soc. Bull.* **1998**, *23*, 44−50.
(3) van Blaaderen, A. *Mater. Res. Soc. Bull.* **1998**, *23*, 39−43.
(4) Denkov, N. D.; Velev, O. D.; Kralchevsky, P. A.; Ivanov, I. B.; Yoshimura, H.; Nagayama, K. *Langmuir* **1992**, *8*, 3183−3190.
(5) Dimitrov, A. S.; Nagayama, K. *Langmuir* **1996**, *12*, 1303−1311.
(6) Kreiger, I. M.; O'Neill, F. M. *J. Am. Chem. Soc.* **1968**, *90*, 3114−3120.
(7) Mirkin, C. A.; Letsinger, R. L.; Mucic, R. C.; Storhoff, J. J. *Nature* **1996**, *382*, 607−609.
(8) Coffer, J. L.; Bigham, S. R.; Li, X.; Pinizzotto, R. F.; Rho, Y. G.; Pirtle, R. M.; Pirtle, I. L. *Appl. Phys. Lett.* **1996**, *69*, 3851−3853.
(9) Alivisatos, A. P.; Johnsson, K. P.; Peng, X.; Wilson, T. E.; Loweth, C. J.; Bruchez, M. P., Jr.; Schultz, P. G. *Nature* **1996**, *382*, 609−611.
(10) Colvin, V. L.; Goldstein, A. N.; Alivisatos, A. P. *J. Am. Chem. Soc.* **1992**, *114*, 5221−5230.
(11) Vossmeyer, T.; DeIonno, E.; R., H. J. *Angew. Chem., Intl. Ed. Engl.* **1997**, *36*, 1080−1083.
(12) Gao, M.; Gao, M. G.; Zhang, X.; Yang, Y.; Yang, B.; Shen, J. *J. Chem. Soc., Chem. Commun.* **1994**, 2777−2778.
(13) van Blaaderen, A.; Ruel, R.; Wiltzius, P. *Nature* **1997**, *385*, 321−324.
(14) Sankaran, V.; Cummins, C. C.; Schrock, R. R.; Cohen, R. E.; Silbey, R. J. *J. Am. Chem. Soc.* **1990**, *112*, 6858−6859.
(15) Hawker, C. J. *Acc. Chem. Res.* **1997**, *30*, 373−382.
(16) Patten, T. E.; Matyjaszewski, K. *Adv. Mater.* **1998**, *10*, 1−15.
(17) Kato, M.; Kamigaito, M.; Sawamoto, M.; Higashimura, T. *Macromolecules* **1995**, *28*, 1721−1723.
(18) Wang, J. S.; Matyjaszewski, K. *J. Am. Chem. Soc.* **1995**, *117*, 5614−5615.
(19) Percec, V.; Barboiu, B. *Macromolecules* **1995**, *28*, 7970−7972.
(20) Bridger, K.; Fairhurst, D.; Vincent, B. *J. Colloid Interface Sci.* **1979**, *68*, 190−195.
(21) Vincent, B. *Chem. Eng. Sci.* **1993**, *48*, 429−436.
(22) Auroy, P.; Auvray, L.; Leger, L. *J. Colloid Interface Sci.* **1992**, *150*, 187−194.

(23) Sunkara, H. B.; Jethmalani, J. M.; Ford, W. T. *Chem. Mater.* **1994**, *6*, 362−364.
(24) Asher, S. A.; Holtz, J.; Liu, L.; Wu, Z. *J. Am. Chem. Soc.* **1994**, *116*, 4997−4998.
(25) Espiard, P.; Guyot, A. *Polymer* **1995**, *36*, 4391−4395.
(26) Bourgeat-Lami, E.; Lang, J. *J. Colloid Interface Sci.* **1998**, *197*, 293−308.
(27) Barthet, C.; Hickey, A. J.; Cairns, D. B.; Armes, S. P. *Adv. Mater.* **1999**, *11*, 408−410.
(28) Ejaz, M.; Yamamoto, S.; Ohno, K.; Tsujii, Y.; Fukuda, T. *Macromolecules* **1998**, *31*, 5934−5936.
(29) Huang, X.; Doneski, L. J.; Wirth, M. J. *Anal. Chem.* **1998**, *70*, 4023−4029.
(30) Husseman, M.; Malmstrom, E. E.; McNamara, M.; Mate, M.; Mecerreyes, D.; Benoit, D. G.; Hedrick, J. L.; Mansky, P.; Huang, E.; Russell, T. P.; Hawker, C. J. *Macromolecules* **1999**, *32*, 1424−1431.
(31) Philipse, P.; Vrij, A. *J. Colloid Interface Sci.* **1989**, *128*, 121.
(32) Iler, R. K. *The Chemistry of Silica: Solubility, Polymerization, Colloid and Surface Properties, and Biochemistry*; John Wiley and Sons: New York, 1979.
(33) Auroy, P.; Auvray, L.; Leger, L. *Physica A* **1991**, *172*, 269−284.
(34) Matyjaszewski, K.; Patten, T. E.; Xia, J. H. *J. Am. Chem. Soc.* **1997**, *119*, 674−680.
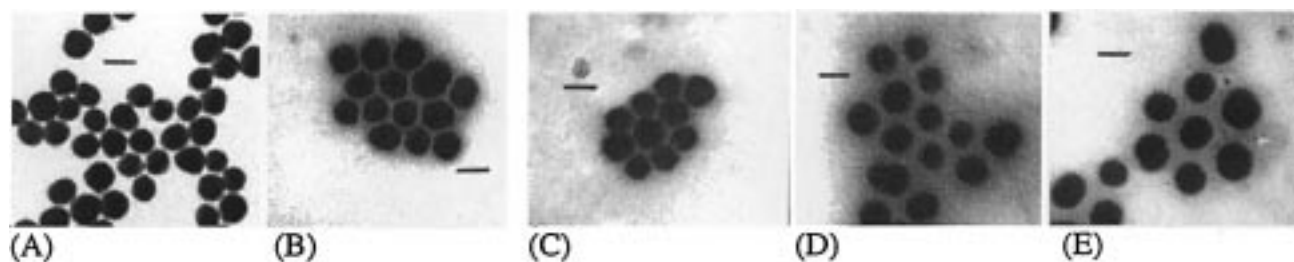
Figure 1. TEM micrographs of the samples from Table 1. Micrographs A through E: high magnification views of samples 1 through 5, respectively (each size bar = 100 nm). Lower magnification micrographs of samples 1 through 5 can be found in the Supporting Information.

Table 1. Data for the Polymerization of Styrene with the CDES-Modified Silica Nanoparticles

	sample no.				
	1	2	3	4	5
polymerization conv (%)	5.7	9.7	30.0	47.3	58.8
DLS av diameter (nm)	75.4	88.5	114	140	188
expected M_n of arms	3000	5050	15600	24600	30600
exptl M_n of arms (GPC)	5400	9000	16800	24600	26500
M_w/M_n of arms (GPC)	1.92	1.32	1.24	1.26	1.33

^{a} Conditions: 1.00 g of CDES-modified nanoparticles (0.14 mmol); [CuCl]$_0$ (47.3 mM), [dNbipy]$_0$ = 94.0 mM (dNbipy = 4,4′-di(5-nonyl)-2,2′-bipyridyl), [styrene]$_0$ = 5.88 M, and *p*-xylene solvent at 130 °C.

hydrodynamic diameters are consistent with a single layer of densely grafted polystyrene chains attached to the surface of the nanoparticles. Portions of the samples were dissolved in toluene and treated with 5% aqueous HF and Aliquot 336, a phase transfer catalyst, to etch the silica cores and to isolate the grafted polymer chains. The molecular weight (M_n) of the grafted polymer, as determined with GPC, increased with polymerization conversion (Table 1), and the molecular weight distributions (M_w/M_n) remained narrow after the initial stages of the polymerization (Table 1). The molecular weights were higher than expected initially, but at later conversions they correlated well with the expected values based upon the initial ratio of monomer to surface initiator sites. The higher-than-expected molecular weights during the initial stages of the polymerization were not observed in analogous polymerizations conducted with benzyl chloride as the initiator. This observation may be a consequence of confinement of the CDES initiator to the surface of the nanoparticle where it cannot freely difuse through the solution. Because molecular weight control in ATRP is derived from the persistent radical effect,[34] some radical termination occurs during the incipient stage of the polymerization. With the confined initiator radicals, most likely uncontrolled polymerization proceeds until the polymeric radical can terminate with another radical either on the surface of the same nanoparticle or on another nanoparticle. The former termination mode seems to occur in these polymerizations, because if interparticle coupling had occurred, then one would have expected to observe through DLS measurements a significant increase in average particle size at low conversions. Taken together, the experimental data were consistent with a controlled/living radical polymerization of styrene from the surface of the silica nanoparticle to yield individual particles comprised of a silica core and a well-defined, densely grated outer polystyrene layer.

Figure 1 shows TEM micrographs of the nanoparticle samples cast from dilute THF solutions. The hybrid nanoparticles formed during the early stages of the polymerization (micrograph A) resembled the unaggregated starting nanoparticles, presumably because the amount and molar mass of the surface-grafted polymer were small. At higher polymerization conversions, the nanoparticles agglomerated upon evaporation of the solvent (micrographs B and C) into domains in which the polystyrene bridged the space between the particles. This agglomeration was most likely assisted by chain entanglement of the higher molar mass polymer chains upon evaporation of the solvent. At the highest polymerization
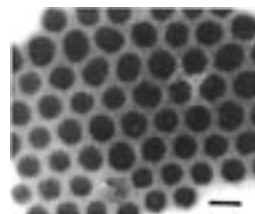

Figure 2. TEM micrograph of a hybrid polystyrene/79 nm SiO$_2$ nanoparticle sample in which the size distribution of the starting silica nanoparticles was 10% (size bar = 100 nm).

conversions (micrographs D and E) the particles again formed domains consisting of a continuous matrix of polystyrene with the silica nanoparticles evenly dispersed throughout. By comparing micrographs B and C with D and E, one can observe that the distance between the nanoparticles within the domains increased from approximately 10 nm to 30 and 40 nm, respectively, in correlation with the molar mass of the grafted polystyrene chains. This observation demonstrates how using a controlled/living polymerization method to prepare the polymer grafts provides a handle through which the morphology of the film can be manipulated. When this synthesis was repeated with starting silica nanoparticles that had a narrow size distribution (<10%), the nanoparticles within the film domains were observed to pack into hexagonal arrays (Figure 2). Auroy et al.[37] concluded that crystalline packing of polymer-grafted colloidal spheres should be observed when the polymer chains are of a high molar mass and a low polydispersity. Because these two conditions were met in the sample shown in Figure 2, the ordered packing of the nanoparticles was observed.

In conclusion, structurally well-defined polymer−nanoparticle hybrids were prepared by modifying the surface of silica nanoparticles with initiators for ATRP and by using these initiator-modified nanoparticles as macroinitiators. Well-defined polystyrene chains were grown from the nanoparticle surfaces to yield individual particles comprised of a silica core and a well-defined, densely grafted outer polymer layer. When cast from solution, the hybrid nanoparticles formed domains in which the inorganic cores were evenly dispersed throughout the polymer matrix. When the starting silica core had a narrow size distribution, the resulting film domains exhibited hexagonal ordering of the silica cores. Such polymer grafting methods may prove useful for generating nanoparticle film arrays with interesting magnetic and optical properties.

Supporting Information Available: Experimental procedures for all syntheses and polymerizations, DRIFT spectra of the starting and CDES-modified nanoparticles, TEM/SEM micrographs of the CDES-modified nanoparticles, lower magnification TEM micrographs of the samples shown in Figure 1, and IR spectra of the silica−polystryrene nanoparticles and the grafted polystyrene isolated after HF etching of the silica core (PDF). This material is available free of charge via the Internet at http://pubs.acs.org.

JA991108L